J Mater Sci (2008) 43:1619–1623
DOI 10.1007/s10853-007-2313-3

Morphology and luminescent properties of Al^{3+}/Mg^{2+}-doped $Y_2O_3:Eu^{3+}$ phosphor

Zhen Liu · Yang Feng · Dongmei Jiao · Na Zhang · Huan Jiao

Received: 6 December 2006 / Accepted: 13 November 2007 / Published online: 25 December 2007

Abstract Al^{3+}/Mg^{2+} doped Y_2O_3:Eu phosphor was synthesized by the glycine-nitrate solution combustion method. In contrast to Y_2O_3:Eu which showed an irregular shape of agglomerated particles (the mean particle size >10 μm), the morphology of Al^{3+}/Mg^{2+} doped Y_2O_3:Eu crystals was quite regular. Al^{3+}/Mg^{2+} substituting Y^{3+} in Y_2O_3:Eu resulted in an obvious decrease of the particle size. Meanwhile, higher the Al^{3+}/Mg^{2+} concentration, smaller the particle size. In particular, the introduction of Al^{3+} ion into Y_2O_3 lattice induced a remarkable increase of PL and CL intensity. While, for Mg^{2+} doped Y_2O_3:Eu samples, their PL and CL intensities decreased. The reason that causes the variation of PL and CL properties for Al^{3+} and Mg^{2+} doped Y_2O_3:Eu crystals was concluded to be related to sites of Al^{3+} and Mg^{2+} ions inclined to take and the difference of ion charge.

Introduction

The performance improving of flat panel displays (FPDs) needs phosphors with high resolution and efficiency [1]. However, so far most field emission displays (FEDs) still adopt the conventional cathode ray tubes (CRTs) phosphors because of the lack of red, green, and blue phosphors with good efficiency at low voltage [2]. In order to satisfy the requirement of FEDs, new types of phosphors should be found or the properties of the conventional phosphors should be improved. Our team focuses on the latter [3–6].

Recently, the measures of incorporating rare-earth co-dopants [3, 7, 8] or non-rare-earth co-dopants [9, 10] into the phosphors were frequently taken to improve the phosphors' properties. The roles of rare earth co-dopants were generally believed to be related to the processes of energy transfer, up-conversion and cross relaxation [11]. However, the role of non-rare-earth co-dopants has not been established, though these phenomena have been reported in several papers. Shin et al. [12] studied Zn-doped Y_2O_3:Eu which was considered to be a potential red phosphor applied to field emission displays. It was found that the cathodoluminescence of the Zn-doped Y_2O_3:Eu phosphor was increased by introducing Zn^{2+} ion into the dead layers. In reference [11], the PL of Y_2O_3:Eu thin film phosphor with Mg^{2+} and Al^{3+} co-doping was investigated and it was found that at a certain concentration, both Mg^{2+} and Al^{3+} co-dopants further enhanced the PL emission intensity. Doping selenium ion (Se^{2+}) into $ZnGa_2O_4$:Mn phosphor could enhance the emission intensity by increasing the average grain size and surface roughness [13]. Lithium ion (Li^+) doping was beneficial to produce well-crystallized $Gd_{2-x}Y_xO_3:Eu^{3+}$ particles with spherical morphology at lower annealing temperature [14] and reduce the density of grain boundaries [15]. Doping Al^{3+} into $Zn_3(BO_3)_2$:Ce improved the luminescent intensity to some extent [16]. Rossner et al. [17] reported that Mg^{2+} and Ti^{4+} additions caused $(Y,Gd)_2O_3:Eu^{3+}$ X-ray luminescence to change. For Mg^{2+} doped system, the luminescent intensity increased whereas Ti^{4+} additions reduced the yield and afterglow of the luminescence. Sun et al. [18] studied the structure and luminescent properties of nanocrystalline Y_2O_3:Eu powders

Z. Liu · Y. Feng · N. Zhang · H. Jiao (✉)
Key Laboratory of Macromolecular Science of Shaanxi Province, School of Chemistry and Materials Science, Shaanxi Normal University, Xi'an 710062, Shaanxi Province, China
e-mail: jiaohuan@snnu.edu.cn

D. Jiao · H. Jiao
China Petroleum and Chemical Corporation, Luoyang Company, Luoyang 471012, China

doped with different metal ions. The doping of Al^{3+} and Mg^{2+} made the PL intensity of nanocrystalline Y_2O_3:Eu powders decreased greatly. Moon et al. [19] found that the brightness of Y_2O_3:Eu powder was improved when Al^{3+} was added.

Y_2O_3:Eu was selected as one candidate for FEDs because of its high brightness, acceptable atmospheric stability and reduced degradation under applied voltages. Many researches focused on the improving of its luminescent intensity [11, 12, 14, 17]. In the present article, the influence of Al^{3+} and Mg^{2+} ions on the PL and CL intensities of Y_2O_3:Eu was investigated. It was found that both of the PL and CL intensities of Al^{3+} ion-doped samples increased in comparison with the undoped ones. On the contrary, by introducing Mg^{2+} ion into Y_2O_3:Eu, both the PL and CL intensities decreased. Particle size and shape were all found to be related to the doping elements and doping contents.

Experimental

Synthesis

We use the glycine-nitrate solution combustion method [18] to synthesize our samples. The starting materials for our synthesis were Eu_2O_3 (purity > 99.99%), Y_2O_3 (purity > 99.99%), $Al(NO_3)_3 \cdot 9H_2O$ (purity > 99%), $(MgCO_3)_4 \cdot Mg(OH)_2 \cdot 6H_2O$ (purity > 99%), and glycine (purity > 99%). First, a transparent solution was obtained by dissolving the stoichiometric amounts of rare-earth oxides, $Al(NO_3)_3 \cdot 9H_2O$ or $(MgCO_3)_4 \cdot Mg(OH)_2 \cdot 6H_2O$ into the dilute nitric acid. Second, glycine was added to the above solution with appropriate ratio. Then, the mixed solution was gradually heated until excess free water evaporated and became sticky. Then, it began burning. The self-combustion lasted for a few seconds. After that, the resultant ashes were calcined at 900 and 1,500 °C for 2h, respectively, then the samples were finally obtained. For all samples the formula $(Y_{0.97-x}M_xEu_{0.03})_2O_3$ ($M = Al^{3+}$ or Mg^{2+}) was used to represent the composition, in which x was the dopant concentration. The concentrations of the dopant ions in the synthesized phosphors were examined by chemical method. The results were well consistent with that of the starting materials.

Characterizations

The crystal structure of all samples was checked by a Rigaku D/max 2000 X-ray powder diffractometer. The PL intensity was measured by using a Hitachi F4500 fluorescence spectrophotometer and the function of energy calibration was applied for the spectral data collections. The CL intensity measurements were conducted by using an YFC-2 cathode luminescence spectrophotometer. The voltage of the electron beam was 10 kV and the current density was 1 μA/cm^2. The emission energy in the visible light range was integrated to represent the luminescent intensity. The particle morphology of the final powders was investigated with a scanning electron microscope (SEM, Philips-FEI Quanta 200).

Results and discussion

Figures 1 and 2 showed the XRD patterns of Mg^{2+} and Al^{3+} doped $(Y_{0.97-x}M_xEu_{0.03})_2O_3$. The XRD patterns were all coincident with the JCPDS card (No.88-1040) with no additional peaks which implied that the Al^{3+} and Mg^{2+} dopants were well incorporated into the structure of Y_2O_3. This result was similar to that of reference [11].

Figure 3 showed the fluorescence spectra of $(Y_{0.97-x}Al_xEu_{0.03})_2O_3$ ($x = 0$, 0.01, 0.03, 0.05). Obviously, the radiation was dominated by the red emission peak centered at 611 nm, which was attributed to the $^5D_0 \rightarrow {}^7F_2$ transition of Eu^{3+}. The sharp emission peak and the absence of spectrum shift might be due to the shielding effect of electrons in the 4f orbit by the outer 5s and 5p orbits, because of which the crystal field had less influence on the emission spectra of rare-earth luminescent centers [11]. For the Mg^{2+} doped samples, the emission spectra were similar to that of the Al^{3+} doped ones.

The inset in Fig. 3 showed the variations of PL intensity with Al^{3+} contents in the system of $(Y_{0.97-x}Al_xEu_{0.03})_2O_3$. The emission intensity was greatly enhanced by Al^{3+} doping, and about 40% increase was observed for $(Y_{0.94}Al_{0.03}Eu_{0.03})_2O_3$. Higher doping concentration of

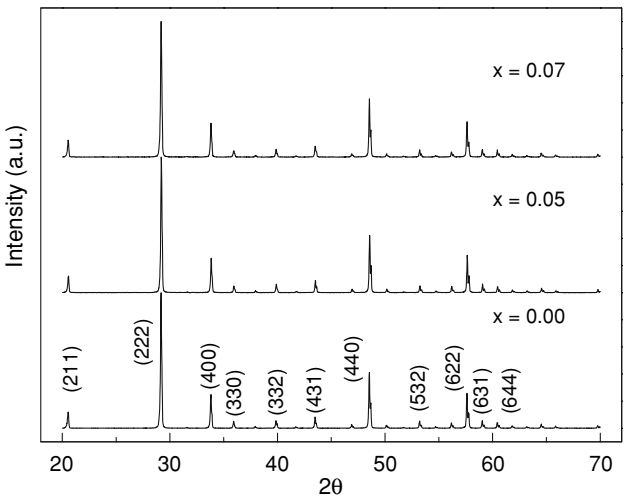

Fig. 1 XRD patterns of $(Y_{0.97-x}Al_xEu_{0.03})_2O_3$ ($x = 0$, 0.05, 0.07)

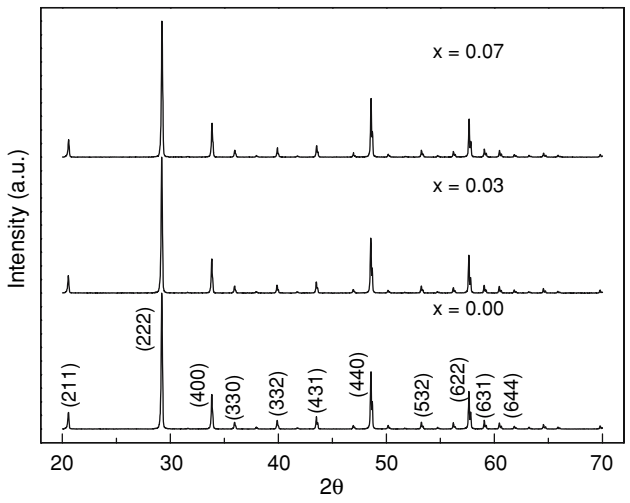

Fig. 2 XRD patterns of $(Y_{0.97-x}Mg_xEu_{0.03})_2O_3$ (x = 0, 0.03, 0.07)

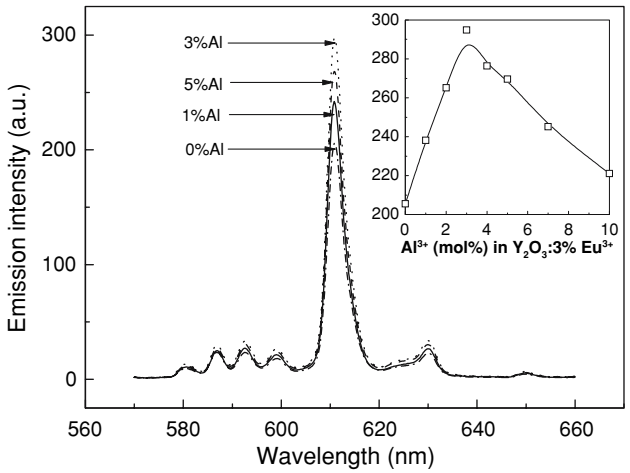

Fig. 3 Fluorescence spectra of $(Y_{0.97-x}Al_xEu_{0.03})_2O_3$ ($x = 0$, 0.01, 0.03, 0.05)

Al^{3+} ion will also quench the fluorescence as shown in Fig. 3.

Figure 4 presented the effect of Mg^{2+} content on the luminescent intensity of $(Y_{0.97-x}Mg_xEu_{0.03})_2O_3$. Different from the Al^{3+} doped ones, the PL intensities of Mg^{2+} doped samples decreased with the increasing of Mg^{2+} ion content.

The crystal structure of Y_2O_3 belongs to the cubic system with space group Ia3. Yttrium occupies two crystallographic sites, C_2 and S_6. The ratio of C_2 to S_6 is 3:1 [20]. The intensity ratio of the $^5D_0 \rightarrow {}^7F_2$ (611–630 nm) to the $^5D_0 \rightarrow {}^7F_1$ ($\sim$590 nm) transition is higher in the site with C_2 symmetry than that in the site with S_6. As reported in previous literatures [21], the effective ionic radii of Al^{3+} and Mg^{2+} ions are 0.51 and 0.66 Å, respectively, both are smaller than that of Y^{3+} ion (0.89 Å). It is instead expected that Al^{3+} ion are introduced into C_2 sites with higher population in the lattice. The sites offered for Eu^{3+} ions have lower symmetry, which

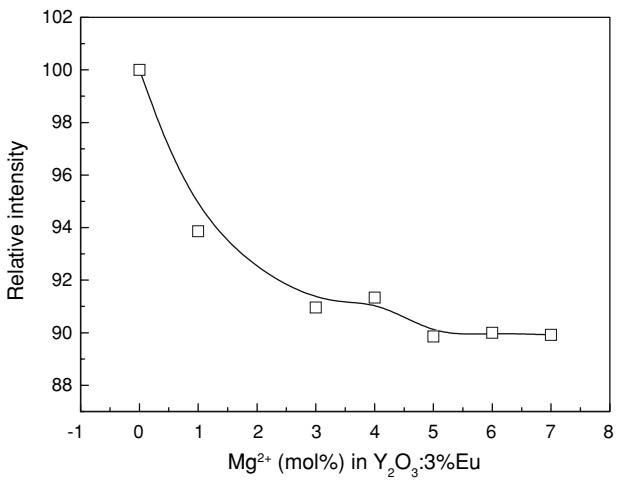

Fig. 4 Effect of Mg^{2+} content on the luminescent intensity of $(Y_{0.97-x}Mg_xEu_{0.03})_2O_3$

is able to lift the parity selection rule and result in the enhanced luminescent properties. So it can be found that for Al^{3+} doped Y_2O_3:Eu, its luminescent intensity is enhanced and ratio of the $^5D_0 \rightarrow {}^7F_1$ to the $^5D_0 \rightarrow {}^7F_2$ transition (I_{592}/I_{611}) decreased slightly with the increasing of Al^{3+} content (as shown in Table 1). That is, increase in the 611 nm peak in Al^{3+} ion doped samples resulted in enhancement of red color and in color coordinate change toward the red region.

But for Mg^{2+} doped samples, the luminescent intensity decreased with the increasing of Mg^{2+} concentration, the ratio of I_{592}/I_{611} showed a tendency of increase. This indicated the doping of Mg^{2+} ion changed the color coordinate toward the orange region. This phenomenon might be related to the charge difference between Y^{3+} and Mg^{2+} ion. For Mg^{2+} doping Y_2O_3:Eu phosphor, replacement of Y^{3+} by Mg^{2+} ion gave defective structure. The charge equilibrium in the lattice was destroyed. In order to maintain the charge balance, an amount of oxygen vacancies emerged. The vacancies might be the energy traps which could increase the nonradiative transition and reduce the luminescent intensity. With the gradual increase in Mg^{2+} content, the vacancies of host lattice greatly increased which would destroy the crystallinity and led to the luminescence quenches.

Table 1 Intensity ratio of the 592 nm peak to the 611 nm of the PL spectrum for various doping contents

Al^{3+} contents	0	1	3	5	7	9	10
I_{592}/I_{611}	0.1141	0.1136	0.1123	0.1120	0.1133	0.1137	0.1141
Mg^{2+} contents	0	1	3	4	5	6	9
I_{592}/I_{611}	0.1141	0.1146	0.1157	0.1167	0.1180	0.1201	0.1201

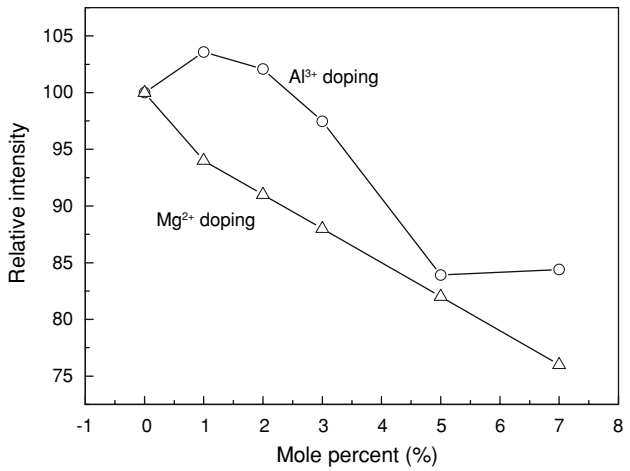

Fig. 5 CL intensity as a function of the Al^{3+}/Mg^{2+} content

Figure 5 showed the CL intensity as a function of Al^{3+}/Mg^{2+} content. For the Al^{3+} doped samples, with the gradual increasing of Al^{3+} concentration, the CL intensity first increased and then decreased. The maximum CL intensity of Al^{3+} ion doped samples appeared at 1% Al^{3+} concentration, which was 1.04 times of the Y_2O_3:Eu phosphor. For the Mg^{2+} doped samples, the CL intensity showed a tendency of persistent decrease.

The optimized chemical composition, particle size distribution, and morphology are necessary requirements for the advanced luminescent materials. Al^{3+} and Mg^{2+} ions doping improved the particle morphology greatly. Figure 6 was SEM micrograph of $(Y_{0.97-x}M_xEu_{0.03})_2O_3$ (M = Al^{3+} or Mg^{2+}). It can be observed that the morphology and grain size were different for various doping concentrations. The image of $(Y_{0.97}Eu_{0.03})_2O_3$ indicated an irregular shape. The particle size was in the range of 10–20 μm, as shown in Fig. 6a. With the increasing of Al^{3+} and Mg^{2+} ions doping concentration, the morphology and dispersion of the particles improved gradually. For $(Y_{0.96}Al_{0.01}Eu_{0.03})_2O_3$ sample, it has a sheet-like morphology with a dimension of 5 μm, which were aggregated by tiny cubes. For $(Y_{0.92}Al_{0.05}Eu_{0.03})_2O_3$, particle size decreased to about 1 μm. For the $(Y_{0.94}Mg_{0.03}Eu_{0.03})_2O_3$ samples, square plate near 5 μm can be observed. For $(Y_{0.92}Mg_{0.05}Eu_{0.03})_2O_3$, particle size decreased to 1 μm. Compared with the $(Y_{0.97}Eu_{0.03})_2O_3$, the edge of grains was clearer and the aggregation among particles was less. It is worth noting that the average particle size decreased with the increasing of Al^{3+}/Mg^{2+} ion doping content.

Some public literatures [11, 18, 19] were also worked on Al^{3+}/Mg^{2+} ion doped in Y_2O_3:Eu phosphor. Some public literatures [11, 18] worked on nano Y_2O_3:Eu and Y_2O_3:Eu thin film. The crystallinity of those samples in the two references was very low. It is not surprising that their luminescent intensity was also very low. People could only

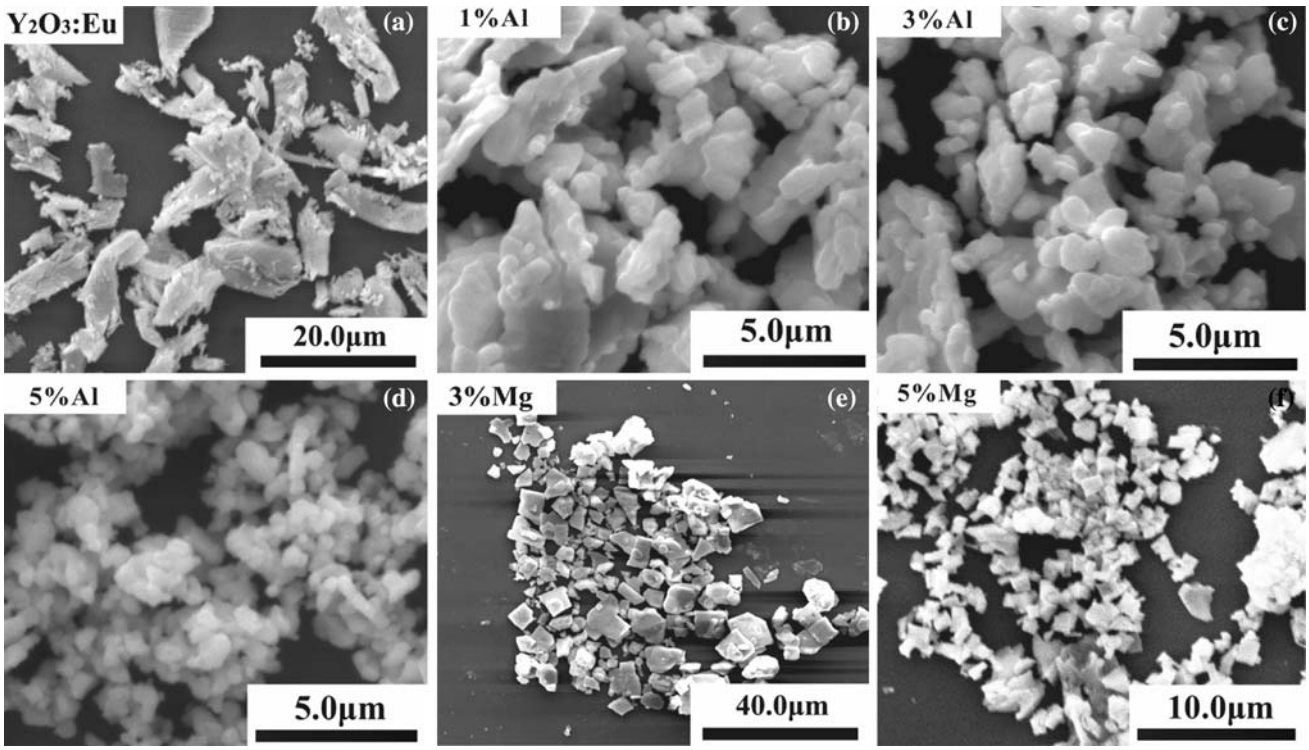

Fig. 6 SEM micrograph of $(Y_{0.97-x}M_xEu_{0.03})_2O_3$ (M = Al^{3+}, Mg^{2+}) (**a**) Y_2O_3:Eu; (**b**) 1% Al^{3+} doped; (**c**) 3% Al^{3+} doped; (**d**) 5% Al^{3+} doped; (**e**) 3% Mg^{2+} doped; (**f**) 5% Mg^{2+} doped

get very limited structure information because diffraction peaks was rather broaden and shifted. So results of those two papers cannot compare with ours. Park et al. [19] found that doping of Al^{3+} could enhance the luminescent intensity; this result was similar to ours. However, change in morphology caused by doping has not been discussed. Our work is a good supplement to it.

Conclusion

In conclusion, a significant change of morphology induced by Al^{3+} and Mg^{2+} doping could also influence PL and CL efficiency in $(Y_{0.97}Eu_{0.03})_2O_3$ phosphor. The doping of Al^{3+} enhanced both PL and CL intensity. For Mg^{2+} doped ones, luminescent properties decreased obviously. Site preference of Al^{3+}/Mg^{2+} in Y_2O_3:Eu and structural vacancies caused by charge difference might be the reasons of variation of luminescent properties.

Acknowledgements We are thankful for the financial support from the State Key Program for Basic Research of China (G1998061308), the National Nature Science Foundation of China (20221101), and the Nature Science Foundation of Shaanxi Province (2004B31).

References

1. Sun LD, Qian Ch, Liao ChSh, Wang XL, Yan ChH (2001) Solid State Commun 119:393
2. Jaskie JE (1996) Mater Res Bull 21:59
3. Jiao H, Liao FH, Tian ShJ, Jing XP (2004) J Electrochem Soc 151(7):H39
4. Jiao H, Wei LQ, Zhang N, Zhong M, Jing XP (2007) J Euro Cer Soc 27:185
5. Jiao H, Wang XJ, Ye Sh, Jing XP (2007) J Luminesc 122–123:113
6. Jiao H, Zhang N, Jing XP, Jiao DM (2007) Opt Mater 29:1023
7. Ank TK, Minh LQ, Vu N, Houng TT, Huong NT, Barthon C, Strek W (2003) J Luminesc 102–103:391
8. Gouveia-Neto AS, da Costa EB, dos Santos PV, Bueno LA, Ribeiro SJL (2003) J Appl Phys 94:5678
9. Bosze EJ, Hirata GA, Shea-Rohwer LE, Mckittrick J (2003) J Luminesc 104:47
10. Jeong JH, Bae JS, Yi SS, Park JC, Kim YS (2003) J Phys Condens Matter 15:567
11. Chong MK, Pita K, Kam CH (2004) Appl Phys A 79:433
12. Shin SH, Kang JH, Jeon DY, Choi SH, Lee SH, You YC, Zang DS (2005) Solid State Commun 135:30
13. Jeong JH, Moon BK, Seo HJ, Bao JS, Yi SS, Kim IW, Park HL (2003) Appl Phys Lett 83:1346
14. Ko MG, Park JC, Kim DK, Byeon SH (2003) J Luminesc 104:215
15. Yi SS, Bae JS, Moon BK, Jeong JH, Park JC, Kim IW (2002) Appl Phys Lett 81:3344
16. Zou WG, Lü MK, Gu F, Wang SF, Zhou GJ, Xiu ZL, Xü HY (2005) Mater Letter 59:1020
17. Rossner W, Jermann F, Ahne S, Ostertag M (1997) J Luminesc 72–4:708
18. Sun BJ, Song HW, Lu ShZh, Yu XL (2003) J Rare Earths 21(Suppl):33
19. Moon HR, Ahn BT, Han JI, Park YK (1999) J Korean Phys Soc 35:S452
20. Park JCh, Moon HK, Kim DK, Byeon SH, Kim BCh, Suh KS (2000) Appl Phys Lett 77:2162
21. Shannon RD (1976) Acta Cryst A32:751